# THE DESIGN AND MANUFACTURING OF THE DYNAMOMETER FOR MEASURING CUTTING FORCES

## VASILE CIOFOAIA, GHEORGHE BEJINARU-MIHOC

Transilvania University of Brasov

**Abstract**: In the engineering applications, in order to measure the force values within a desired precision range there are needed specific design and manufacturing conditions and dynamometers sufficient measuring accuracy. In this paper, we used a Strain Gage based dynamometer design, a tree component, a computer linked design; tests were carried out to measure the cutting forces. This dynamometer can be used in static and dynamic force measurements in cutting machines. It has been noted that the cutting forces recorded synchronously from the tests have corresponded to the calculated values.

Keywords: cutting force, strain gage, dynamometer, mechanical cutting

#### 1. INTRODUCTION

Force modeling in metal cutting is important for a multitude of purposes, including thermal analysis, tool life estimation, chatter prediction, and tool condition monitoring.

Numerous approaches have been proposed to model metal cutting forces with various degrees of success [1, 2, 3, 4].

In addition to the effect of work piece materials, cutting parameters, and process configurations, cutting tool thermal properties can also contribute to the level of cutting forces. Significant efforts have been devoted to understanding the force profiles in metal cutting.

Along with a laborious experimental approach, several numerical and analytical approaches have been proposed to model the chip formation forces [4] and the associated cutting forces.

Analytical models have been favored for the modeling of forces in metal cutting because they are easy to implement and because they can give much more insight about the physical behavior in metal cutting.

### 2. THE CUTTING FORCE

Large forces are generated during the machining process, which are shown in figure 1. Analytical models have been favored for the modeling of forces in metal cutting .

To model the chip formation forces in metal cutting, two fundamental approaches have been extensively researched: minimum energy principle [3] and slip line

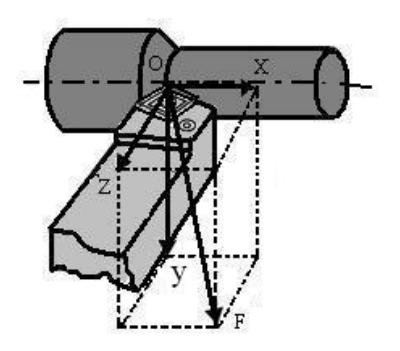


Fig.1 Cutting force directions

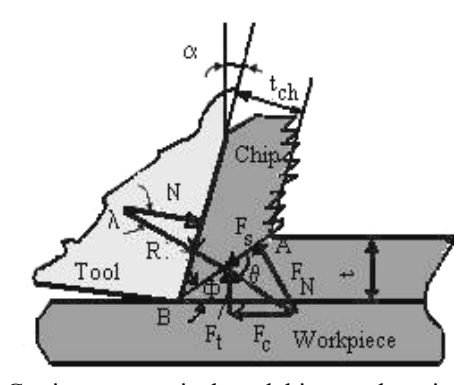


Fig.2 Cutting geometrical model in metal cutting

field theory.

The former assumes that the plastic deformation occurred uniformly in the shear plane only so that the cutting energy can be calculated from the shear strain and stress at the shear plane.

Minimizing this energy with respect to the shear angle yields the direction of the shear plane [3, 4].

The forces are generated during the machining process are shown in figure 2. The cutting force  $F_f$  acts in the direction of the cutting velocity (X) and the thrust force  $F_t$  act normal to the cutting velocity in the direction perpendicular to the work piece (Y). The basic force relationships can be given as:

$$F_{f} = R\cos(\lambda - \alpha); F_{t} = R\sin(\lambda - \alpha); F_{c} = l_{AB}lw; F = R\sin\lambda;$$

$$N = R\cos\lambda; R = \frac{F_{s}}{\cos\theta} = \frac{k_{AB}tw}{\sin\phi\cos\theta}; t_{ch} = \frac{\cos(\phi - \alpha)}{\sin\phi}t;$$
(1)

where R is the resultant force, the vector sum of the cutting force and thrust force, can be used to define the relation between the normal cutting force  $F_{\rm N}$  and shear cutting force  $F_{\rm c}$ ; l is length of AB(length of shear band),  $\alpha$  – rake angle,  $\lambda$  – frictional angle between R and N, w – depth of cut.

### 3. FORCE MEASUREMENT

The force components in lathe turning can be measured in three directions, as shown in figure 1.

The determine the force values, octagonal rings are used. The ring shape is shown in figure 3. The thickness t, radius r and width of circular ring b are the three basic parameters which control the effect the rigidity and sensitivity.

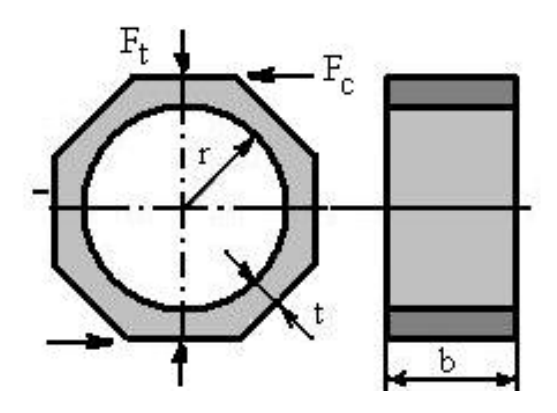


Fig. 3 Octagonal ring dimensions

Width b is considered to be 20 mm in order to be able to mount the electric translator. The material features are yield strength 600-900 N/mm<sup>2</sup>, Young modulus  $E = 2,1.10^5 N/mm^2$ , contraction coefficient v = 0.3 and hardness 217 HB. Taking into account dimensions as seen in figure 3 (b = 20 mm, t = 4 mm and r = 16 mm), the forces  $F_t$  and  $F_c$  produce the deformations  $\varepsilon_t$  and  $\varepsilon_c$ that can be determined as:

$$\varepsilon_t = \pm \frac{1.09 F_t r}{Ebt^2}; \quad \varepsilon_c = \pm \frac{2.18 F_c r}{Ebt^2}$$
 (2)

The determined tension values are within the safety limits since

$$\sigma_t = E\varepsilon_t \ \sigma_c = E\varepsilon_c$$
.

The next figures present the displacement results and the tension values determined for the  $F_t$  force.

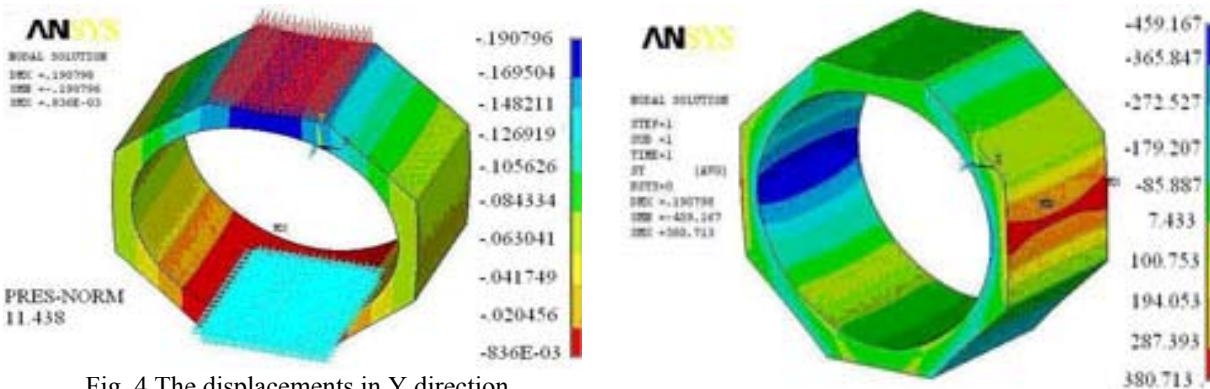


Fig. 4 The displacements in Y direction

Fig. 5 The stresses in Y direction

The placement for the TER captors on the four elastic elements in order to determine the  $F_{\rm f}$ ,  $F_{\rm c}$  forces and the  $M_{\rm Fx}$  momentum is presented in Fig. 6. In the Wheatstone bridge all the mounting found at the level of the tensiometric marks develop under the influence of the bending moment modifications of the afferent  $\Delta R_i$ 

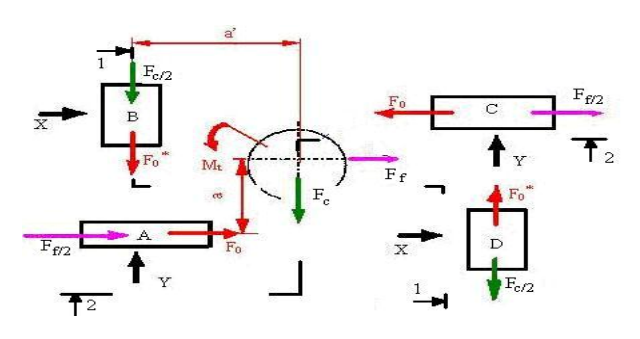


Fig. 6 The positioning of the four elastic elements noted A, B, C and D [1, 2]

resistance.

The effect of axial or cutting force is eliminated due to the device design. The  $\Delta U$  tension disequilibrium is proportional to the alimentation tension, in continuous or alternative current.

The cumulative effects will be:

$$\frac{U_e}{U_i} = \frac{K_{TER}}{4} \left( \sum \varepsilon_j \right) \tag{3}$$

where:  $U_e$  is the output tension for the Wheatstone bridge, Ui is the input tension for the Wheatstone bridge,  $K_{TER}$  –TER constant,  $K_{TER} = 2,10$  the index for the Wheatstone bridge is

$$\varepsilon^* = \frac{4}{K_{ap}} \cdot \frac{U_e}{U_i} \tag{4}$$

where:  $\varepsilon^*$  is the indication for the tensiomentric

bridge,  $K_{\text{ap}}\!-\!$  the K factor of the device,  $K_{\text{ap}}\!\!=\!2$  . Thus it follows that

$$\varepsilon^* = \frac{4}{K_{ap}} \cdot \frac{K_{TER}}{4} \left( \sum \varepsilon_j \right) = \frac{K_{TER}}{K_{ap}} \cdot \sum \varepsilon_j = \frac{1}{c} \sum \varepsilon_j$$
 (5)

where:

$$c = \frac{K_{ap}}{K_{TEP}} \tag{6}$$

The  $\varepsilon_i$  value can be determined from the formula:

$$\varepsilon_{j} = \frac{\sigma_{j}}{E} = \frac{1}{E} \cdot \frac{M_{jz}}{W_{z}} = \frac{1}{E} \cdot \frac{n_{j} \cdot F}{W_{z}} \tag{7}$$

where: F is the load for the octagonal ring;  $n_j$  – is the load coefficient;  $M_{jz}$  – the bending moment at the TER level. It follows that the  $\varepsilon^*$  value can be computed from the relation:

$$\varepsilon^* = \frac{1}{c} \left( \sum \cdot \frac{1}{E} \cdot \frac{n_j \cdot F}{W_z} \right) \tag{8}$$

The thrust force  $F_t$  is supported by the A, B, C and D rings of the dynamometer as shown in figure 6. The thrust force affects the strain gauges 3, 4, 7, 8, 11, 12, 15 and 16. Among these strain gauges, the gauges 3, 7, 11 and 15 are subject to tensile stress, while the gauges 4, 8, 12 and 16 are subjected to compressive stress. The feed force  $F_t$  is supported by the A and C rings as shown in figure 7. The strain gauges designed to measure the feed force are mounted on the outer surface of the A and C rings. The main cutting force  $F_c$  is supported by the B and D rings as shown in figure 8. The main cutting force affects the strain gauges 9, 10, 13 and 14.

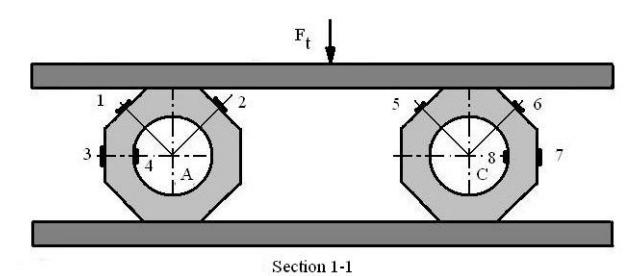


Fig. 7 The strain gauges on the ring A and C – section 1-1 (fig.6)

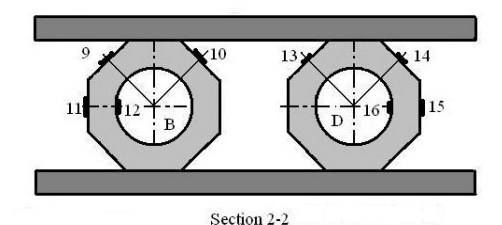


Fig.8 The strain gauges on the ring B and D
- section 2-2 (fig.6)

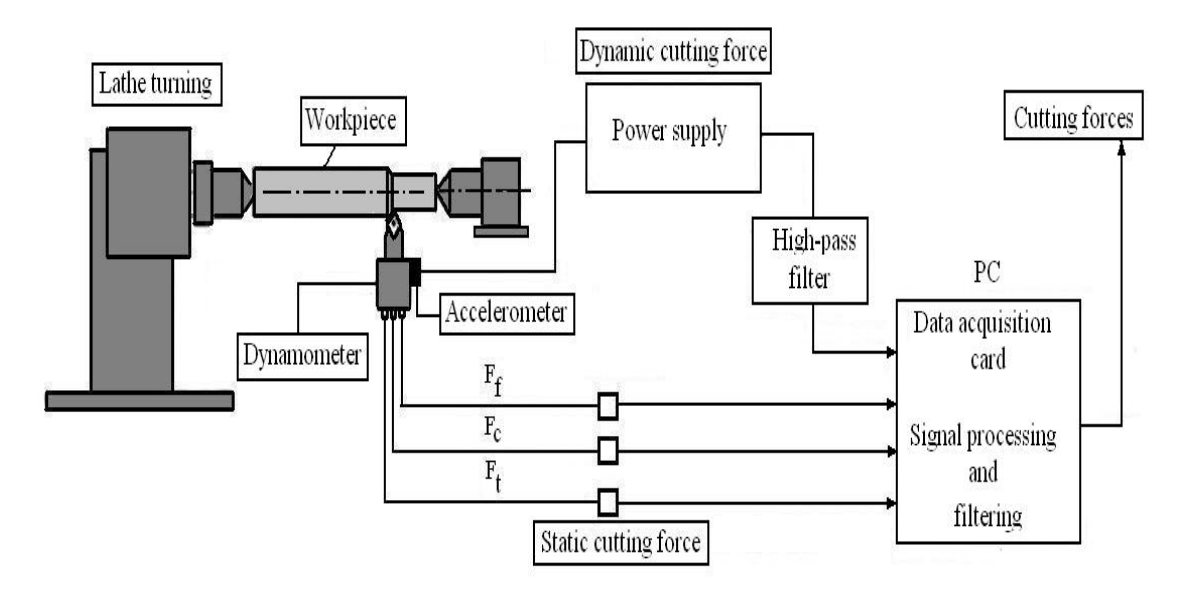


Fig. 9. Schematic representation of experimental set-up

Figure 9 presents the schematic diagram of the cutting force measurement system. The dynamometer calibration was performed for the forces  $F_{\rm f}$ ,  $F_{\rm t}$  and  $F_{\rm c}$  up to 2600 N from 50 N to 50 N. The forma of the dynamometer is showed in figure 10 [6]. Figure 11 shows the calibration curves for thurst force. Similar, it can obtained the curves for feed force and main cutting force respectively.

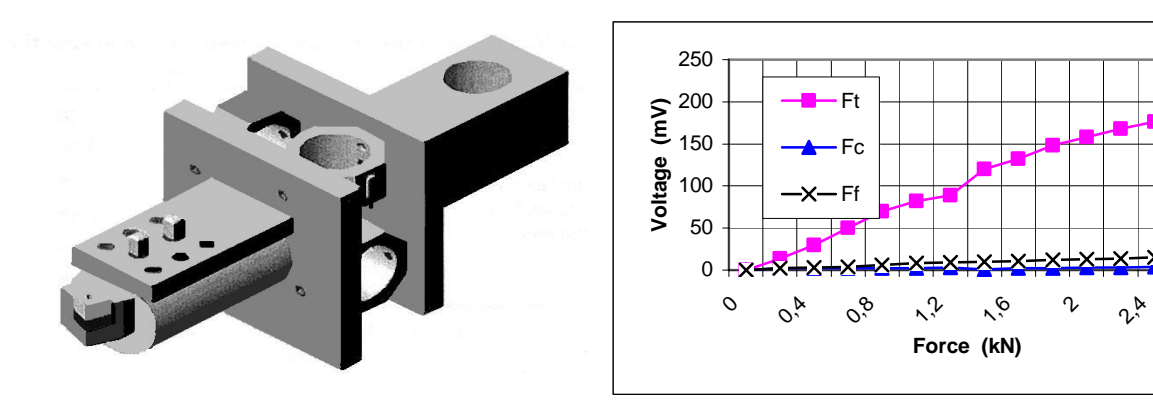


Fig. 10 Dynamometer [6]

Fig.11 Calibration curve for thurst force  $(F_t)$ 

## 4. CONCLUSIONS

The dynamometer can measure a cutting force on three directions in the same time during the cutting process. The values can be acquired and stored by a computer by using a data acquisition system. This dynamometer is designed to measure forces up to 3500 N. It can be statically or dynamically calibrated.

## REFERENCES

- [1] Bejinaru Mihoc, Gh., "Tehnologia producției microsistemelor", Ed. Univ Transilvania Brașov, 2002.
- [2] Bejinaru, Gh., "Tehnologia mecanicii fine și mecatronicii", vol. 1, Reprografia Universității Transilvania Brașov, 1991
- [3] Ciofoaia, V. Botis, M. Dogaru, Fl., Curtu, I., Metoda elementelor finite. Editura Infomarket Braşov, 2001
- [4] Kalhori V. *Modelling and Simulation of mechanical Cutting. Doctoral thesis.* Lulea University of Technology. Sweden, 2001
- [5] Wince, J. N.,. *Modelling chip formation in orthogonal metal cutting using finite element analysis*. Mississippi State University, 2002.
- [6] Şeker, U., Kurt, A, Çiftçi, I., *Design and construction of a dynamometer for measurement of cutting force with linear motion.* Mat.Des.2002, 23, p355 360..